

Absence of magnetic pair breaking in Zn-doped $\text{YBa}_2\text{Cu}_3\text{O}_7$

R. E. Walstedt, R. F. Bell, L. F. Schneemeyer, and J. V. Waszczak
AT&T Bell Laboratories, Murray Hill, New Jersey 07974

W. W. Warren, Jr.
Department of Physics, Oregon State University, Corvallis, Oregon 97331

R. Dupree and A. Gencten
Department of Physics, University of Warwick, Coventry CV4 7AL, United Kingdom
 (Received 21 April 1993)

$^{63}\text{Cu}(2)$ NMR linewidths in Zn-doped $\text{YBa}_2\text{Cu}_3\text{O}_7$ exhibit a predominant component proportional to T^{-1} in the normal state. We attribute this result to spin-exchange scattering of carriers from localized moments associated with Zn impurities in the CuO_2 planes. The estimated moment-carrier exchange, $J_{\text{eff}}=20$ meV, is more than an order of magnitude too small to account for the suppression of T_c in this system via Abrikosov-Gorkov pair breaking. A suggested alternative explanation is pair breaking by strong potential scattering from the Zn impurity sites which requires d -wave pairing.

Of the many experimental routes to a better understanding of the mechanism of superconductivity in the cuprates, one of the most promising involves the effects of substitutional impurities on the copper sites. Certain impurities including Zn have surprisingly strong effects on the value of the superconducting transition temperature, T_c (Ref. 1) of $\text{YBa}_2\text{Cu}_3\text{O}_7$ (YBCO), while others such as Al and Ga are much less disruptive of the superconducting state. In the case of Zn, replacement of 3% of the Cu, i.e., $\text{YBa}_2(\text{Cu}_{0.97}\text{Zn}_{0.03})_3\text{O}_{7.0}$, is sufficient to reduce T_c from 92 K to about 60 K.²⁻⁴ At 10% Zn substitution superconductivity is destroyed altogether. Although various workers are not unanimous on the point, a number of structural investigations⁵⁻⁹ indicate that Zn substitutes primarily on the Cu(2) sites (CuO_2 planes). This contrasts with the trivalent impurities Al and Ga which substitute mainly on the Cu(1) sites (CuO chains).¹⁰ The relative effectiveness of Zn in destroying superconductivity can be attributed in part to Zn substitution on the planar sites, where it is widely believed that the superconductivity resides.

Magnetic susceptibility studies¹¹ indicate the presence of local moment (Curie law) paramagnetism in Zn-doped YBCO, with inferred local-moment concentrations comparable with that of the Zn. The presence of such moments has been invoked to explain increased nuclear relaxation rates⁸ and Curie-like line-broadening effects^{12,13} observed in ^{89}Y NMR studies of this system, as well as to suggest magnetic pair breaking^{8,12} as the cause for the suppression of T_c . It is, however, noteworthy that Co,^{12,13} Al,¹³ and Ga,¹³ which substitute on the Cu(1) site, are also found to produce Curie-like ^{89}Y broadening effects, while having a much smaller effect on T_c . In order to clarify the situation regarding the Zn-doping effects, we have undertaken detailed ^{63}Cu NMR studies of Zn-, Al-, and Ga-doped YBCO, which are presented in this paper. Results on the highly documented Cu NMR in this system enable us to quantify the effects that local moments have on carriers in the CuO_2 planes. A

detailed analysis of our results leads to, among other things, a quantitative estimate of the Abrikosov-Gorkov pair breaking for the case of Zn doping.

In accord with the site preferences noted above, Al and Ga are found to broaden primarily (and severely) the Cu(1)-site NMR line, whereas Zn substitution broadens both Cu(1) and Cu(2) lines. Given the strong tendency for Cu(1) to broaden with any kind of disorder,^{14,15} these effects are consistent with the site assignments mentioned. The Zn doping also leads to both a significant loss of Cu(2) NMR intensity ("wipeout") as well as a striking T^{-1} temperature dependence for the Cu(2) linewidth. The latter effect can be understood in terms of RKKY-like spin-density oscillations in the CuO_2 planes driven by exchange between the mobile carriers and localized moments associated with the Zn sites. Using the indirect nuclear spin-spin coupling in undoped $\text{YBa}_2\text{Cu}_3\text{O}_7$ as a calibration^{16,17} we present a quantitative analysis of moment-carrier exchange couplings below. The results are then used to discuss various exchange-related effects in the Zn-doped material.

The samples used for these experiments were prepared at Warwick University using conventional solid-state reaction techniques¹³ and were found to be single phase up to 10% Zn substitution and to at least 7% Al. The normal-state susceptibility of the 3% Zn-doped sample was measured up to room temperature in order to estimate the concentration of localized moments. For nuclear quadrupole resonance (NQR) studies, the powdered samples were sealed under an oxygen atmosphere in glass ampoules. After completion of the NQR spectra and relaxation measurements, the material was removed, mixed with epoxy, and oriented in a 7.5 T magnetic field for NMR measurements.

In order to investigate the effects of metal substitution on Cu-site spin dynamics, we have measured ^{63}Cu spin-lattice relaxation at the Cu(1) and Cu(2) sites in Zn, Al, and Ga-doped $\text{YBa}_2\text{Cu}_3\text{O}_7$ using ^{63}Cu NQR.¹⁸ The Cu(1) and Cu(2) NQR lines at 22.1 and 31.5 MHz, respectively,

are broadened appreciably in the doped samples compared with pure $\text{YBa}_2\text{Cu}_3\text{O}_7$, especially on the low-frequency side of the lines. The peak frequencies in the NQR spectra exhibited little temperature dependence, unlike pure YBCO,¹⁹ and our spin-lattice relaxation measurements were carried out at fixed frequencies of 31.5 and 22.1 MHz over the temperature range 60–300 K.

In the case of samples containing 3% Zn, 2.5% Al, and 2.5% Ga, a small deviation from single exponential T_1 recovery was noted. Nevertheless, these data could be fitted with a single exponential function to obtain average values, \overline{T}_1 , which can be compared with the corresponding values found in nominally pure YBCO. Values of $1/(\overline{T}_1 T)$ for our 3% Zn-doped sample are compared with the corresponding results for pure $\text{YBa}_2\text{Cu}_3\text{O}_7$ in Fig. 1 (circles). These data show that $1/(\overline{T}_1 T)$ is reduced for both Cu(1) and Cu(2) sites in the 3% Zn material. Relative to the rates in undoped materials, the reduction at the Cu(1) sites is slightly greater than at the Cu(2) sites. Nevertheless, the temperature dependence at both sites remains very similar to that of the corresponding site in undoped material. This behavior is completely unlike that observed in undoped, but oxygen-deficient material with a comparable reduction in T_c . The T_1 behavior with T is very different in the latter case²⁰ from that of $\text{YBa}_2\text{Cu}_3\text{O}_7$, the relaxation rate at 300 K being actually greater than that of the 90 K phase. In contrast with the Zn-doped material, measurements on the 2.5% Al and Ga samples yielded relaxation rates for Cu(2) sites within experimental error of those measured in pure YBCO while the Cu(1) rates were reduced significantly more than in Zn-doped material. These points are illustrated in Fig. 1 with T_1 data for the 2.5% Al-doped sample (squares). Our main conclusion here is that for the majority of Cu(2) spins the mechanism of spin-lattice relaxation enhanced by antiferromagnetic fluctuation effects in

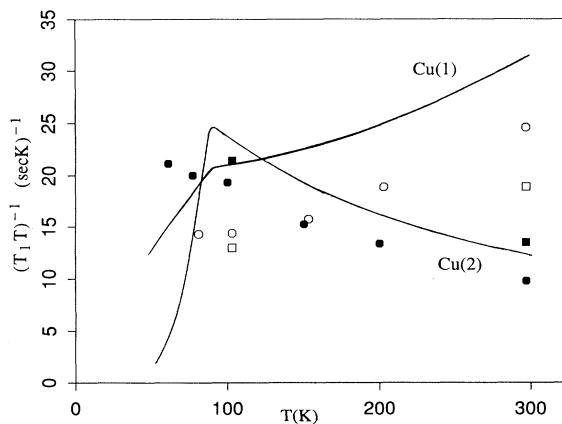


FIG. 1. Temperature dependence of $1/(\overline{T}_1 T)$ values obtained from single exponential fits to the spin-lattice relaxation curves for Cu(1) (open points) and Cu(2) (closed points) sites in $\text{YBa}_2(\text{Cu}_{0.97}\text{Zn}_{0.03})_3\text{O}_{7.0}$. Data, obtained by NQR at the respective sites, are shown for $\text{YBa}_2(\text{Cu}_{0.97}\text{Zn}_{0.03})_3\text{O}_7$ (circles) and $\text{YBa}(\text{Cu}_{0.975}\text{Al}_{0.025})_3\text{O}_7$ (squares). The solid lines represent measured values of $1/\overline{T}_1 T$ in undoped $\text{YBa}_2\text{Cu}_3\text{O}_7$.

the CuO_2 planes^{21–23} is only slightly affected by the 3% Zn doping. We also note that if spin fluctuations provide the coupling mechanism for high- T_c superconductivity, as has been proposed,²⁴ then the T_1 results (Fig. 1) show that T_c is highly sensitive to small changes in the fluctuation spectrum.

⁶³Cu NMR spectra for the 3% Zn-doped YBCO are shown in Fig. 2 for four temperatures above T_c . The dominant features of these spectra are the central ($\frac{1}{2} \leftrightarrow -\frac{1}{2}$) transitions for Cu(1) and Cu(2) and the first-order ($\pm\frac{1}{2} \leftrightarrow \pm\frac{3}{2}$) quadrupolar satellite for Cu(1).²⁵ The spectra exhibit complex temperature dependence, but the main point is that the Cu(2) line broadens rapidly as T is reduced, whereas the Cu(1) features change more gradually. These observations together with the strong intensity of the Cu(1) lines relative to the Cu(2) are in sharp contrast with our observations in a 2.5% Al-doped sample (not shown). In that case, the Cu(2) line broadened only slightly on cooling from 300 to 100 K while the Cu(1) line broadened until it was almost indistinguishable from the broad background caused by the quadrupolar satellites. The latter effect is even more severe than observed for $\text{YBa}_2\text{Cu}_3\text{O}_{6.7}$ (Ref. 14) and, as expected, is consistent with impurities occupying chain sites.¹⁰

Because the Cu(1) ($\pm\frac{1}{2} \leftrightarrow \pm\frac{3}{2}$) satellite spectra overlap the Cu(2) central ($\frac{1}{2} \leftrightarrow -\frac{1}{2}$) transition, it is necessary to separate these line intensities in order to analyze quantitatively the Cu(2) central line. It is important to note that the Cu(1) satellite line shape is determined by first-

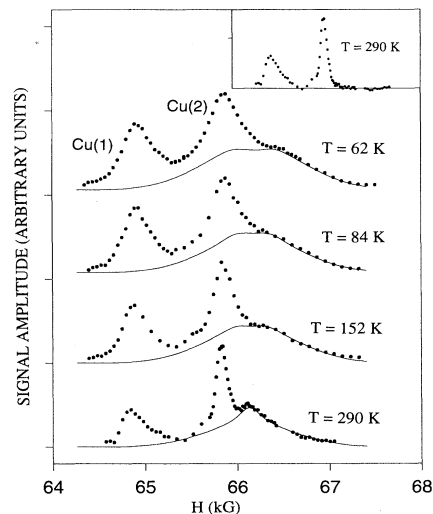


FIG. 2. Field-swept NMR spin-echo spectra taken at 75.3 MHz for oriented 3% Zn-doped $\text{YBa}_2\text{Cu}_3\text{O}_7$ powder at various temperatures in the normal state. The strong peak at 65.9 kG is identified at the $\frac{1}{2} \leftrightarrow -\frac{1}{2}$ transition of the Cu(2) sites. The peak just below 65 kG is the $\frac{1}{2} \leftrightarrow -\frac{1}{2}$ transition for the Cu(1) sites while the broad line just above (and beneath) the Cu(2) line is attributed to the $\pm\frac{1}{2} \leftrightarrow \pm\frac{3}{2}$ quadrupolar satellites of the Cu(1) sites.²⁵ The solid line is a fit to the Cu(1) satellites used to obtain corrected spectra for the Cu(1) and Cu(2) $\frac{1}{2} \leftrightarrow -\frac{1}{2}$ lines. The corrected spectrum at room temperature is shown in the inset.

order quadrupolar broadening. The c -axis electric field gradient (EFG) component V_{cc} for the Cu(1) is very small ($\eta \approx 1$) as a result of almost exact cancellation of competing contributions, and is extremely sensitive to small variations of the bond lengths with temperature. Furthermore, the profile of the satellites is almost perfectly symmetrical about a point determined by the (known) c -axis NMR shift. Thus, by fitting the high-field side of the satellite spectrum, we determine the satellite intensity in the region of overlap as well. The modeled Cu(1) satellite lines are shown by the solid lines in Fig. 2. The change of this line-shape profile with temperature results from changes in V_{xx} and/or V_{yy} of $< 1\%$. Subtraction of the modeled satellites from the observed spectra yields corrected Cu(2) central transition lines (see inset, Fig. 2).

The full widths at half maximum ΔH_{FWHM} for the resulting Cu(2) line profiles are plotted as a function of T^{-1} in Fig. 3. These data exhibit very nearly linear behavior, confirming the expected T^{-1} temperature dependence of RKKY broadening. This linewidth is an order of magnitude greater than what would be expected from dipolar fields alone. The Cu(1) width is temperature independent at high temperatures, rising abruptly between 84 and 62 K. It is not clear that this is caused by the local moments, as low-temperature broadening for the Cu(1) sites is typically seen even in high-quality undoped samples.^{14,15}

We interpret the linewidth data from Fig. 3 using a formulation of the local-moment-induced spin-density oscillations closely following that in Ref. 16. The central element in this calculation is the real part of the susceptibility $\chi'(\mathbf{q}, 0) \equiv \chi'(\mathbf{q})$, which has been modeled for YBCO as discussed in Refs. 17, 22, and 23. The principal unknown parameter to be evaluated is the exchange between a local

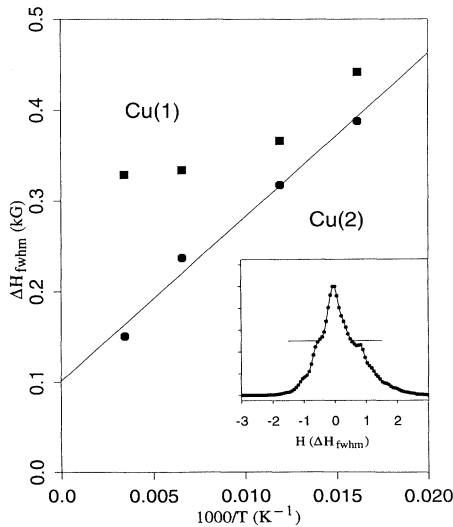


FIG. 3. Linewidth ΔH_{FWHM} of the corrected Cu(2) (dots) and Cu(1) (squares) central ($\frac{1}{2} \leftrightarrow -\frac{1}{2}$) transitions vs inverse temperature in 3% Zn-doped $\text{YBa}_2\text{Cu}_3\text{O}_7$. The solid line shown is a linear regression on the Cu(2) data. The inset shows the simulated line shape obtained using a Gaussian model for the susceptibility $\chi'(q)$, where the correlation length is $\xi = 1.25a$ (see text).

moment and the mobile carriers in the conduction band. The measured susceptibility at temperatures $65 \text{ K} \leq T \leq 290 \text{ K}$ fits approximately the form $\chi(T) = C_0/T + \chi_{\text{host}}$, where we assume for simplicity that the host background susceptibility χ_{host} is a constant. We find $C_0 = (0.54 \pm 0.1) \text{ Kemu}/(\text{mole Zn})$ and $\chi_{\text{host}} = (2.0 \pm 0.5) \times 10^{-4} \text{ emu}/(\text{mole f.u.})$. The Curie term corresponds to a local moment with slightly greater than one Bohr magneton for each Zn substitution. We shall assume that the moments are coupled by exchange J to the carrier-moment spins on each of the four Cu(2) sites neighboring a Zn impurity.

In an applied field each localized moment induces a spatially oscillatory static spin density in the surrounding lattice through the agency of an exchange coupling term $H_{\text{ex}} = -J \sum_{\delta(\text{nn})} \mathbf{S}^L \cdot \mathbf{S}(\delta)$, where \mathbf{S}^L is the local-moment spin operator and $\mathbf{S}(\delta)$ is the conduction-band spin operator at a Cu(2) site displaced by a nearest-neighbor vector δ from the Zn site. Using the formalism of Ref. 16 the corresponding static exchange field $\mathbf{H}_{\text{ex}}(\mathbf{q}) = 2J \langle S_z^L \rangle (\cos q_x a + \cos q_y a) / g\mu_B N$ then induces a spin polarization $S_z(\mathbf{q}) = (g\mu_B)^{-1} \chi'(\mathbf{q}) H_{\text{ex}}(\mathbf{q})$, which may be Fourier transformed to obtain the spin density $S_z(\mathbf{r}) = \sum_{\mathbf{q}} S_z(\mathbf{q}) \exp(i\mathbf{q} \cdot \mathbf{r})$. The result for net spin at site $\mathbf{r} = (n_x, n_y)a$ is

$$S_z(n_x, n_y) = - \frac{(-1)^{n_x + n_y} J \langle S_z^L \rangle}{(2\pi g\mu_B)^2} \times \sum_{\delta(\text{nn})} \int_{-\pi}^{\pi} dq_x \int_{-\pi}^{\pi} dq_y \chi'(\mathbf{q}) \times \cos[q_x(n_x + \delta_x)] \times \cos[q_y(n_y + \delta_y)], \quad (1)$$

where the origin in \mathbf{q} space is placed at $\mathbf{q}_{\text{AFM}} = (\pi, \pi)/a$. Taking $\chi'(\mathbf{q})$ to be commensurate, $S_z(n_x, n_y)$ then alternates in sign between neighboring sites. Furthermore, the spin-density oscillations induced at the four nn Cu(2) sites neighboring a Zn site reinforce one another, because these sites all lie on the same antiferromagnetic (AFM) sublattice.

To proceed with our linewidth calculation, we adopt for $\chi'(\mathbf{q})$ the Gaussian form used by Millis, Monien, and Pines²² to interpret T_1 data and also by Imai *et al.*,¹⁷ to model indirect nuclear spin-spin interactions. Thus, $\chi'(\mathbf{q}) = \chi_0 \beta^{1/2} \xi^2 \exp(-q^2 \xi^2)$, where ξ is the correlation length, χ_0 is the host-band uniform susceptibility, and β is a scale parameter.²¹ Substituting, Eq. (1) then gives $S_z = D (-1)^{n_x + n_y} \sum_{\delta(\text{nn})} \exp[-|\mathbf{r} + \delta|^2 / 4\xi^2]$ for the spin density surrounding a single impurity, where the prefactor $D = -\chi_0 \beta^{1/2} J \langle S_z^L \rangle / (16\pi\mu_B^2)$. The corresponding range function for hyperfine fields is then given by $H_z^{\text{hf}}(\mathbf{r}) = A_c S_z(\mathbf{r}) + B \sum_{\delta(\text{nn})} S_z(\mathbf{r} + \delta)$, where we specialize to the case of applied field along the c axis with $A_c = -380 \text{ kG}$ and $B = 92 \text{ kG}$ (Refs. 15 and 26) (hyperfine fields per unit spin). Computer simulation with a 100×100 square lattice having randomly distributed Zn impurities then yields the line profile shown in the inset to Fig. 3, where we have taken $\xi = 1.25a$ from the T_1 fits.²³ The final result for the full width at half

height is

$$\Delta H_{\text{FWHM}} \approx 40\beta^{1/2}|J\rho\langle S_z^L \rangle \text{ kG}, \quad (2)$$

where $\rho = \chi_0/\mu_B^2$ is the band density of states. A critical step is to adopt $\beta^{1/2}\xi/a \approx 13$ from indirect spin-spin coupling measurements.¹⁷ The measured susceptibility gives $\langle S_z^L \rangle = 4.5 \times 10^{-5}H/T$ and the slope of the data in Fig. 3 gives $\Delta H_{\text{FWHM}}T/H_0 = 0.27$ K. With these values Eq. (2) then gives $|J\rho| \approx 0.015$. Using the estimate²² $\rho = 3$ states/eV-both spins, one finally obtains $|J| \approx 5$ meV.

It is rather surprising that such a small exchange interaction can give such a large linewidth effect. This result is attributable to both the ample host density of states and to the very large antiferromagnetic enhancement effect of $\chi''(\mathbf{q})$. We estimate the pair-breaking effect of J using the Abrikosov-Gorkov formula²⁷ $\Delta T_c = c\rho J_{\text{eff}}^2 S(S+1)/\pi k_B$, where ΔT_c is the expected decrease in T_c and J_{eff} is the effective exchange between a local moment and the carrier spins. For this estimate we assume $J_{\text{eff}} \sim 4J = 20$ meV, since the moment interacts with each of four neighboring sites with coupling J . Using $c = 0.045$ for in-plane moments and $S(S+1)$ from the measured Curie constant, we find $\Delta T_c \sim 0.12$ K. This is smaller than the observed effect by a factor ~ 300 , strongly suggesting that magnetic pair breaking is not the

mechanism of T_c suppression. We also note in passing that the standard expression for the Kondo temperature $k_B T_K = D|J_{\text{eff}}\rho|\exp(1/J_{\text{eff}}\rho)$ yields an estimated $T_K < 1$ mK, in keeping with the observed results.

If the above analysis is correct, then it rules out a strongly suspected mechanism for the suppression of T_c in YBCO caused by Zn doping. However, if superconductivity in this system is of d -wave symmetry, ordinary potential scattering will have a pair-breaking effect, as shown by Millis, Sachdev, and Varma.²⁸ Transport data⁴ demonstrate that potential scattering is very strong for Zn impurities in YBCO, leading to the possible conclusion that this scattering causes the suppression of T_c . On the other hand, it seems it would be very difficult to explain the T_c suppression on the basis of s -wave symmetry, since our results show that the density of states is affected very little by the Zn doping. Recently, low-temperature T_1 studies,²⁹⁻³² as well as penetration depth measurements,³³ and other results for the superconducting state of YBCO (Refs. 34 and 35) have been put forward in apparent support of d -wave pairing in this system.

The authors would like to thank A. J. Millis for many illuminating discussions and S.E.R.C. for support (R.D.).

¹H. A. Borges *et al.*, *Physica* **148B**, 411 (1987).

²G. Xiao *et al.*, *Phys. Rev. Lett.* **60**, 1446 (1988).

³J. M. Tarascon *et al.*, *Phys. Rev. B* **37**, 7458 (1988).

⁴T. R. Chien, Z. Z. Chang, and N. P. Ong, *Phys. Rev. Lett.* **67**, 2088 (1991).

⁵G. Xiao *et al.*, *Nature* **332**, 238 (1988).

⁶H. Maeda *et al.*, *Physica C* **157**, 483 (1989).

⁷T. Kajitani *et al.*, *Jpn. J. Appl. Phys.* **27**, L354 (1988).

⁸G. Balakrishnan *et al.*, *Physica C* **161**, 9 (1989).

⁹F. Bridges, G. G. Li, J. B. Boyce, and T. Claeson (unpublished).

¹⁰T. Siegrist *et al.*, *Phys. Rev. B* **36**, 7137 (1987).

¹¹C.-S. Gee *et al.*, *J. Superconduct.* **1**, 63 (1988).

¹²H. Alloul *et al.*, *Phys. Rev. Lett.* **67**, 3140 (1991).

¹³R. Dupree, A. Gencten, and D. McK. Paul, *Physica C* **193**, 81 (1992).

¹⁴R. E. Walstedt *et al.*, *Phys. Rev. B* **41**, 9574 (1990).

¹⁵R. E. Walstedt *et al.*, *Phys. Rev. B* **45**, 8074 (1992).

¹⁶C. H. Pennington and C. P. Slichter, *Phys. Rev. Lett.* **66**, 381 (1991).

¹⁷T. Imai, C. P. Slichter, A. P. Paulikas, and B. Veal, *Phys. Rev. B* **47**, 9158 (1993).

¹⁸Y. Kohori *et al.*, *J. Phys. Soc. Jpn.* **57**, 2632 (1988).

¹⁹H. Riesemeier *et al.*, *Jpn. J. Appl. Phys.* **26**, Suppl. 26-3, 2137 (1987).

²⁰W. W. Warren, Jr. *et al.*, *Phys. Rev. Lett.* **62**, 1193 (1989).

²¹N. Bulut *et al.*, *Phys. Rev. B* **41**, 1797 (1990); N. Bulut and D.

J. Scalapino, *Phys. Rev. Lett.* **68**, 706 (1992).

²²A. J. Millis, H. Monien, and D. Pines, *Phys. Rev. B* **42**, 167 (1990).

²³A. J. Millis and H. Monien, *Phys. Rev. B* **45**, 3059 (1992).

²⁴P. Monthoux and D. Pines, *Phys. Rev. Lett.* **69**, 961 (1992); *Phys. Rev. B* **47**, 6069 (1993).

²⁵C. H. Pennington *et al.*, *Phys. Rev. B* **37**, 7944 (1988).

²⁶F. Mila and T. M. Rice, *Physica C* **157**, 561 (1989).

²⁷D. E. MacLaughlin, *Solid State Physics*, edited by H. Ehrenreich, F. Seitz, and D. Turnbull (Academic, New York, 1976), Vol. 31, p. 1.

²⁸A. J. Millis, S. Sachdev, and C. M. Varma, *Phys. Rev. B* **37**, 4975 (1988).

²⁹D. J. Scalapino, *High Temperature Superconductivity*, edited by K. S. Bedell, D. Coffey, D. Meltzer, D. Pines, and J. R. Schrieffer (Addison-Wesley, Reading, MA, 1990), p. 400.

³⁰M. Takigawa, J. L. Smith, and W. L. Hults, *Phys. Rev. B* **44**, 7764 (1991).

³¹J. A. Martindale *et al.*, *Phys. Rev. Lett.* **68**, 702 (1992).

³²N. Bulut and D. J. Scalapino, *Phys. Rev. Lett.* **68**, 706 (1992).

³³W. N. Hardy, D. A. Bonn, D. C. Morgan, R. Liang, and K. Zhang, *Phys. Rev. Lett.* **70**, 3999 (1993).

³⁴D. Thelen, D. Pines, and J. P. Lu, *Phys. Rev. B* **47**, 9151 (1993).

³⁵J. P. Lu, *Bull. Am. Phys. Soc.* **38**, 95 (1993), and references therein.